JOURNAL OF MATERIALS SCIENCE 31 (1996) 1537–1543

Influence of heat treatment on properties of copper-based shape-memory alloy

M. O. LAI, L. LU, W. H. LEE
Department of Mechanical and Production Engineering, National University of Singapore, 10 Kend Ridge Crescent, Singapore 119260

An investigation was performed on a Cu–Zn–Al ternary alloy to examine the influence of heat treatment on its shape-memory effect. Four heat treatments were carried out, namely, step quenching, ice–water quenching, water quenching and glycol quenching from three different temperatures of 800, 850 and 900 °C. It was observed that step-quenched samples showed the best martensitic structure for high resistance to shape-memory degradation. Ice–water quenching induced vacancy-pinning effects and hence lowered transformation temperature and degradation life compared to step quenching. However, no transformation was detected in water and glycol-quenched specimens due to the stabilization of martensite. The results showed that shape-memory effect is strongly influenced by many heat-treatment parameters, such as betatizing temperature, betatizing duration and rate of quenching. Step-quenched specimens also showed a higher number of cycles to failure in comparison to ice-quenched specimens. Owing to the dominating effects of large grain size and martensitic plates, the advantages of step quenching, however, disappeared when a high betatizing temperature of 900 °C was used. Several kinds of defects were observed after fatigue testing, namely microvoids, cracks near martensitic plates, cracks at the interface of inclusions and inside inclusions.

1. Introduction

Cu–Zn–Al shape-memory alloys (SMAs), the most popular being copper-based SMAs because of their low cost, are functional materials whose effects can be best described by their shape change during heating and cooling, and by their superelasticity during loading at elevated temperature. These functions are strongly influenced by heat treatment [1, 2] and may even be lost after prolonged applications due mainly to large elastic anisotropy, large grain size, large orientation dependence of the transformation and also grain-boundary segregation [3–7]. Three types of failure of SMAs during cyclic deformation have been observed [8]:

(a) failure by fracture due to stress or strain cycling at constant temperature;

(b) change in physical, mechanical and functional properties such as transformation temperatures, transformation hysteresis, etc., due to pure thermal cycling through the transformation;

(c) degradation of shape-memory effect due to stress, strain or temperature cycling in or through the transformation region.

Failure of shape-memory effect may be influenced by grain size, density of defects, heat-treatment procedures, amount of deformation, types of deformation applied, and other factors [9].

The purpose of the present work was to investigate the effects of heat-treatment processes and microstructure on the cyclic life of copper-based SMA.

2. Experimental procedure

2.1. Heat treatment

Shape-memory alloy (SMA) wire of 2.5 mm diameter with composition of Cu 17.5 at% Zn 5 at % Al was used in the present study. The wire was cut into specimens of length 150 mm. They were then betatized at three different temperatures of 800, 850 and 900 °C and quenched into four different media, namely, ice–water, water at 26 °C, glycol at 26 and 95 °C, followed by ageing treatment at 95 °C for 1 h in order to stabilize the transformation temperatures. The heat-treatment process is tabulated in Table I. Betatizing durations were 30 and 10 min, respectively, for specimens designated with numbers and with the letter S in Table I. The transformation temperatures of the heat-treated specimens were then measured using a Dupon 910 differential scanning calorimeter (DSC). Microstructure of the heat-treated specimens was examined using optical and Jeol JSM-T300A scanning electron microscopes.

2.2. Shape-memory degradation measurement

Simple bending of the SMA wire specimens in the form of a cantilever beam, as shown in Fig. 1, was performed in monoethylene glycol medium at 120 °C. Pre-deformation strain (minimum deformation strain) of the specimen was 0.05%, while the maximum deformation strain during bending was 0.5%, calculated

0022–2461

TABLE I Heat treatment of shape-memory wire

Specimen	Betatizing temperatures (°C)			Quenching conditions			
	800	850	900	Ice–water	Water at 26 °C	Glycol at 26 °C	Glycol at 95 °C
800IW	•			•			
800W	•				•		
800G	•					•	
800SQ	•						•
850IW		•		•			
850W		•			•		
805G		•				•	
850SQ		•					•
900IW			•	•			
900W			•		•		
900G			•			•	
900SQ			•				•
S800IW	•			•			
S850IW		•		•			
S900IW			•	•			
S800SQ	•						•
S850SQ		•					•
S900SQ			•				•

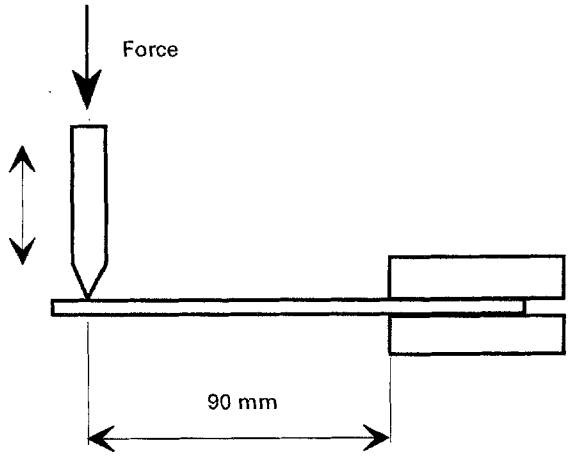

Figure 1 Cantilever beam bending of the test specimen.

using the following equations

$$P = \frac{2\pi D^3 E\varepsilon_x}{64L} \quad (1)$$

and

$$\delta = \frac{PL^3}{3EI} \quad (2)$$

where P is the bending force, ε_x the deformation strain during bending, δ the maximum deflection, E the modulus, I the area moment of inertia, D the diameter of the testing specimen, and L the bending length.

The frequency of bending was controlled at 20 cycles min^{-1}, sufficiently slow to allow time for recovery of stress-induced martensite to the parent phase. Bending was done using a cam system through a follower in contact with the specimen. The number of bends was recorded automatically and terminated once the cam follower separated from the SMA specimen.

After fatigue testing, the specimens were cut using a diamond saw at the position of maximum deformation. They were then gold-coated so that the morphologies of the cross-section of the specimens could be examined using SEM.

3. Results and discussion

3.1. Shape-memory effect

DSC measurements of the heat-treated specimens are shown in Fig. 2. No transformations were detected for the specimens which were quenched in water and glycol at room temperature. From the phase diagram, it is known that the SMA reveals disordered bcc β-phase when it is heated to 800–900 °C. A slow cooling from the parent phase may cause the β-phase to decompose into the equilibrium phases, such as α- and β-phases. To obtain the shape-memory effect, the metastable β-phase must be retained [10]. For the four different quenching rates used in the present work, decomposition could be avoided. However, the direct quenching of a betatized specimen to room temperature, which is close to the M_f temperature at which martensitic transformation finishes, may result in a combination of martensite and untransformed parent phase with disordered atom pairs [9]. During ageing, atoms will undergo rearrangement by a chemical driving force at the expense of free energy of the martensite when transferred to the martensite phase. Therefore, the chemical free energy of the martensite is partially used up for the reordering of a stabilized martensite which leads to a decrease in chemical free energy in the martensite. Owing to the decrease in chemical free energy in the martensite, the martensite becomes more stable and cannot reverse back to the parent phase during subsequent heating. In addition, direct quenching does not allow sufficient time for the excess vacancies to diffuse to the surface or grain boundaries. Vacancies that are not annealed form

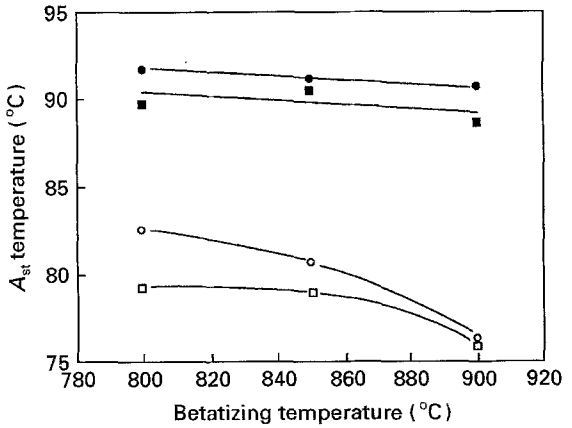

Figure 2 DSC measurements of the SMA wires after different heat-treatment processes: (○, □) long and (●, ■) short betatizing times for (○, ●) ice–water quenching and (□, ■) step quenching.

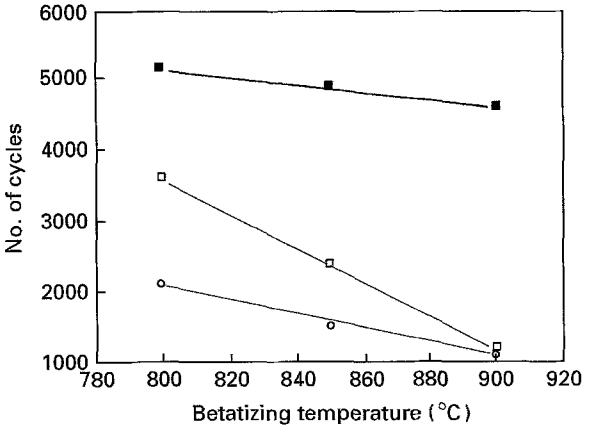

Figure 3 Change in A_{st} temperatures after different heat treatments. The A_{st} temperatures tended to be lower with increase in betatizing temperature. (○, □) Long and (■) short betatizing times, for (○) ice–water and (□, ■) step quenching.

clusters which may pin the martensite plate boundaries and render the reverse transformation more difficult [9]. Step quenching, by which specimens were quenched to a temperature just above the M_s temperature at which martensite transformation starts, however, allows an equilibrium degree of order to be achieved prior to martensitic transformation. Vacancy concentration and quenching stress are also minimized. From DSC curve, it is known that step-quenched specimens possess a shape-memory effect.

Quenching into ice–water results in a completely martensitic phase with no disordered atom pairs. However, excess vacancies are trapped in clusters within the grains. The chemical free energy of the martensite is only slightly influenced by vacancy pinning.

The influence of different heat-treatment processes on the transformation temperature, A_{st}, is depicted in Fig. 3. It can be noted that the reverse transformation temperature is lowered when high betatizing temperature is used. On the other hand, the reverse transformation temperature is delayed when a high quenching rate is employed.

3.2. Fatigue and shape-memory degradation

Fig. 4 shows the number of cycles to failure for the different specimens used in the present study. In general, three phenomena can be observed.

(a) The lower the betatizing temperature, the longer is the degradation life for both ice–water quenching and step quenching;

(b) Step quenching of the SMA wire specimens into 100 °C glycol gives a higher resistance to shape-memory degradation compared to those quenched into ice–water, especially at low betatizing temperatures.

(c) Degradation life of step-quenched specimens decreases faster than that of ice–water quenched specimens when the betatizing temperature is increased.

Quenching into ice–water resulted in a completely martensitic phase with no disordered atom pairs and due to the high quenching rate, the excess vacancies which resist transformation were trapped in clusters within the grains. For specimens that were step-quenched, however, vacancies were minimized because sufficient time was allowed for vacancy diffusion.

It was noted that the advantages associated with step quenching disappeared with the increase in betatizing temperature because the degradation life of step-quenched specimens decayed faster than that of ice–water-quenched specimens. When a betatizing temperature of 900 °C was used, both the water-quenched and the 100 °C glycol-quenched specimens showed approximately the same degradation life. This observation can be explained by the dominating effects of grain growth and large martensitic plates at high temperature.

The betatizing temperature can influence the size of the grains and martensite plate, and the concentration of vacancies which, in turn, affect the resistance of SMA to intergranular failure. Fig. 5 shows the microstructure of the SMA specimens after different betatizing temperatures at a given quenching rate. It is seen that the increase in betatizing temperature is accompanied by an increase in the grain size and martensitic plate size. The martensitic plates are oriented in several directions, resulting in many jagged martensite/martensite impingement boundaries within a SMA grain. The disordered arrangement is characteristic of martensite formed from ice–water quenching. The step-quenched martensitic plates are, in contrast, more uniformly aligned within a grain.

3.3. Microstructure observations

Morphologies of the cross-section of the specimens after fatigue testing are shown in Fig. 6a–h. At least five types of failure can be identified:

(a) defects formed in microvoids as shown in Fig. 6a. It was found that the microvoids were normally formed near the martensitic plates where large accommodation was required by martensitic transformation. It is believed that the formation of microvoids could be due to the motion and accumulation of dislocations during transformation;

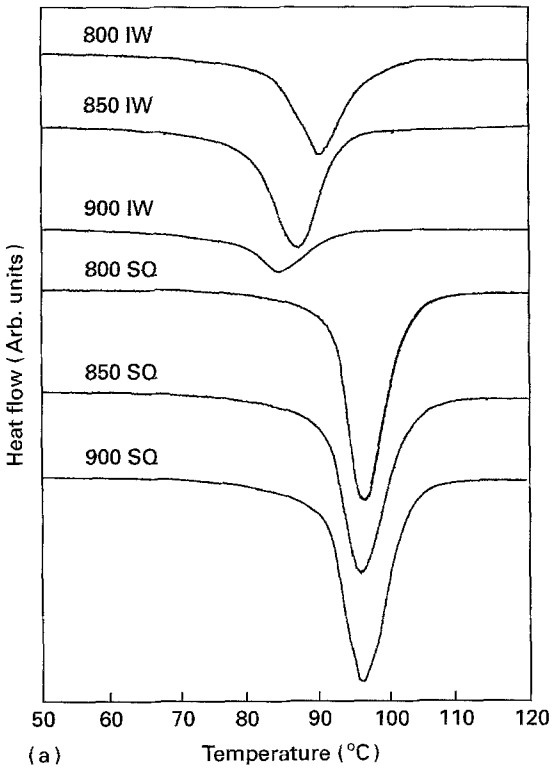

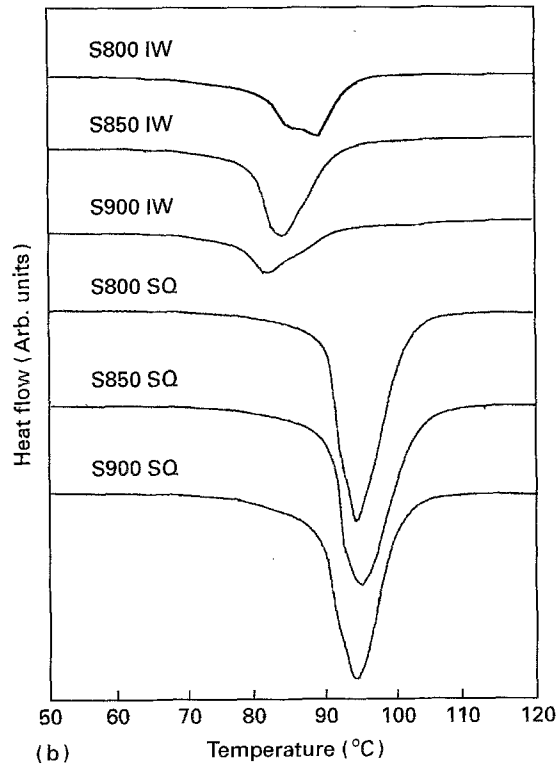

Figure 4(a, b) Fatigue life as functions of betatizing temperature and quenching rates.

(b) cracks initiated from microvoids and propagated along the side of martensitic plates with increase in cycle time as shown in Fig. 6a;

(c) cracks formed near martensite and crossing the martensitic plate as shown in Fig. 6b. No microvoids were observed;

(d) cracks formed at locations with no martensitic plate were observed as shown in Fig. 6c and d. It appears that this type of crack is more serious where no transformation could be seen. The occurrence of such cracks may mostly be due to large deformation during bending. Because there was no transformation locally, large deformation caused by bending had to be tolerated by elastic and/or plastic deformation rather than by martensitic transformation. The strain could be high enough to lead to the formation of cracks. Normally, this type of crack is distributed randomly in the test samples;

(e) cracks between matrix and inclusions which have been used for grain refinement purposes have been observed due to growth of the martensitic plates (Fig. 6e). A high-stress field related to the large orientation dependence of the transformation is believed to have been generated. During bending, a high-stress field can either lead to plastic deformation between matrix and inclusions, or microcracks. In addition to cracking between matrix and inclusions, fracture of inclusions can also be observed, as shown in Fig. 6e and f;

(f) owing to high-temperature and long-term betatizing, oxidation, dezincification and loss of aluminium content occurred on the surface of the SMA wires. EDAX analysis data showed that zinc was about 8 at % and aluminium about 4 at % at the surface. The thickness of this layer was about 30 μm when the 900 °C betatizing temperature was used. These observations implied that the material at the surface layer had already lost its shape-memory behaviour because of low zinc and aluminium contents. During transformation, the surface layer remained untransformed. Hence, the deformation strain at the surface was beyond the elastic range leading to plastic deformation. Below the surface layer, however, the material was still in the elastic region due to martensitic transformation. A high-stress field induced between the surface layer and the core soon led to the formation of cracks between them. This type of defect was only observed when a high betatizing temperature of 900 °C was used, as shown in Fig. 6h.

From the thermodynamic point of view, elastic strain energy is stored in the material due to martensitic transformation induced by bending. This stored strain energy acts as a driving force to assist reverse transformation when the specimen is unloaded. This thermodynamic relationship can be expressed as

$$\Delta G^{m\to p} = \Delta g_{ch} + g_{fri} + g_{ela} \quad (3)$$

where $\Delta G^{m\to p}$ is the chemical driving force, Δg_{ch}, the difference in Gibbs free energies between martensitic phase and parent phase, g_{fri}, the frictional energy, g_{ela}, the stored elastic energy. If local relaxation due either to plastic deformation or to the occurrence of microcracks and microvoids, as shown in Fig. 6a–f, took place, the stored elastic energy of g_{ela} in the martensite will be lowered. Because stored elastic energy assists reverse transformation, the loss of stored elastic energy will consequently stabilize the martensite and finally make reverse transformation more difficult. Some of the martensitic plates cannot reverse to the parent phase upon release of the bending force because of the lack of internal energy.

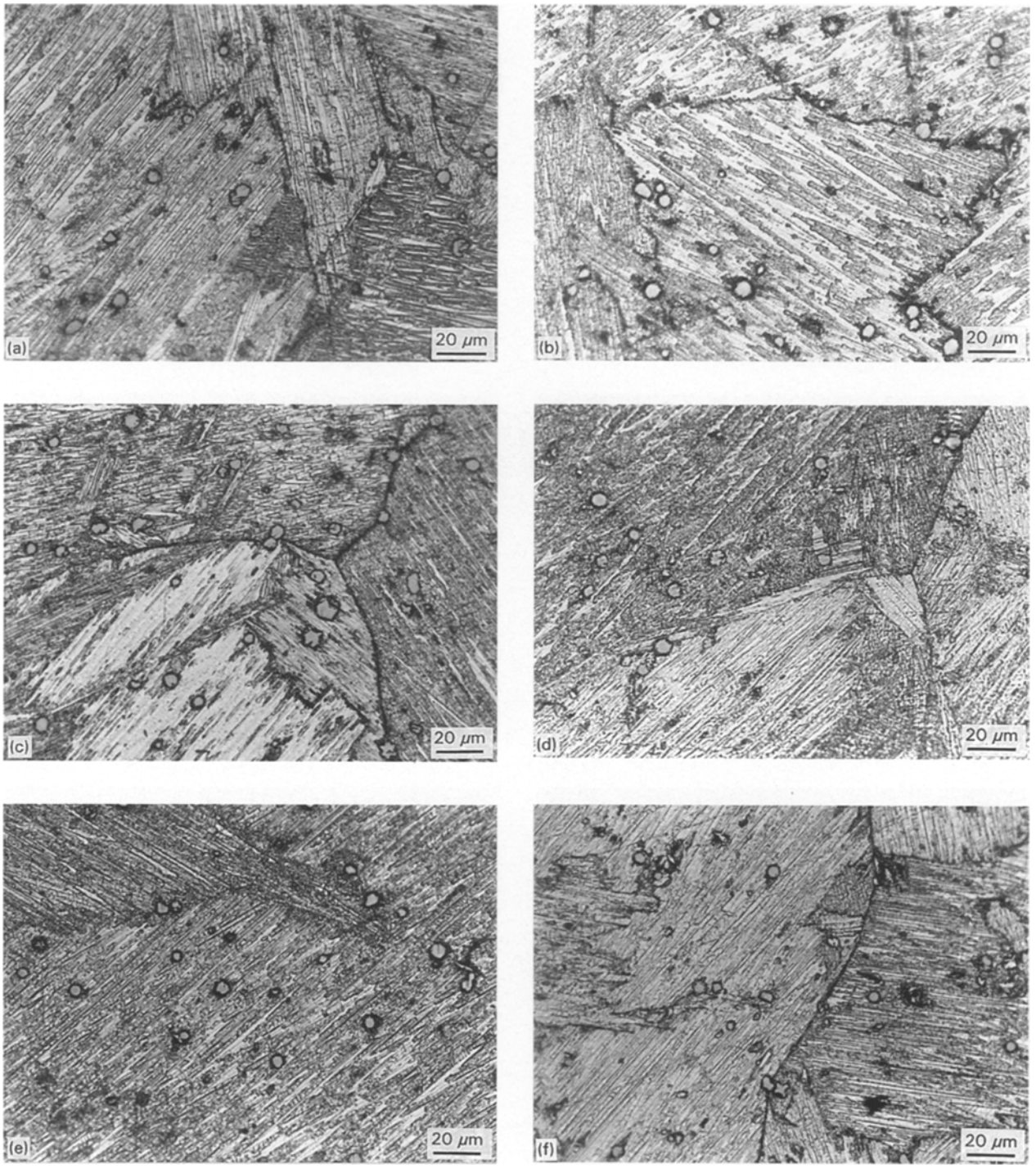

Figure 5 Microstructure of the test specimens after heat treatment. (a–c) Betatized at 800, 850 and 900 °C, respectively, and then quenched into ice–water; and (d–f) betatized at 800, 850 and 900 °C, respectively, and then step-quenched.

The occurrence of irreversible strain may also be due to the following reasons [8, 9, 11–13]:

(a) some amount of irreversible plastic deformation can take place at the beginning of fatigue cycling. The cause of such deformation may be stress accommodation at the parent phase grain boundaries. This phenomenon can occur in all types of quenching media;

(b) cyclic deformation may result in an increase in density and motion of dislocations in the parent phase. Such dislocations are accumulated in bands parallel to the trace given by the habit plane of the induced variant. These also respond in an irreversible manner;

(c) pinning by excess quenched-in vacancies and reordering of the martensite may also occur whereby partial martensite becomes stabilized. The lower degradation life of the ice-quenched specimens may be due to any of the above reasons.

To examine the influence of grain size, another heat treatment at which the betatizing duration was only 10 min, was performed. Owing to the short betatizing duration, smaller grain size and martensitic plates were obtained. From Fig. 4, it can be seen that the degradation life is dramatically increased. It is noted that degradation life is not strongly affected by the betatizing temperature if a short betatizing duration is employed.

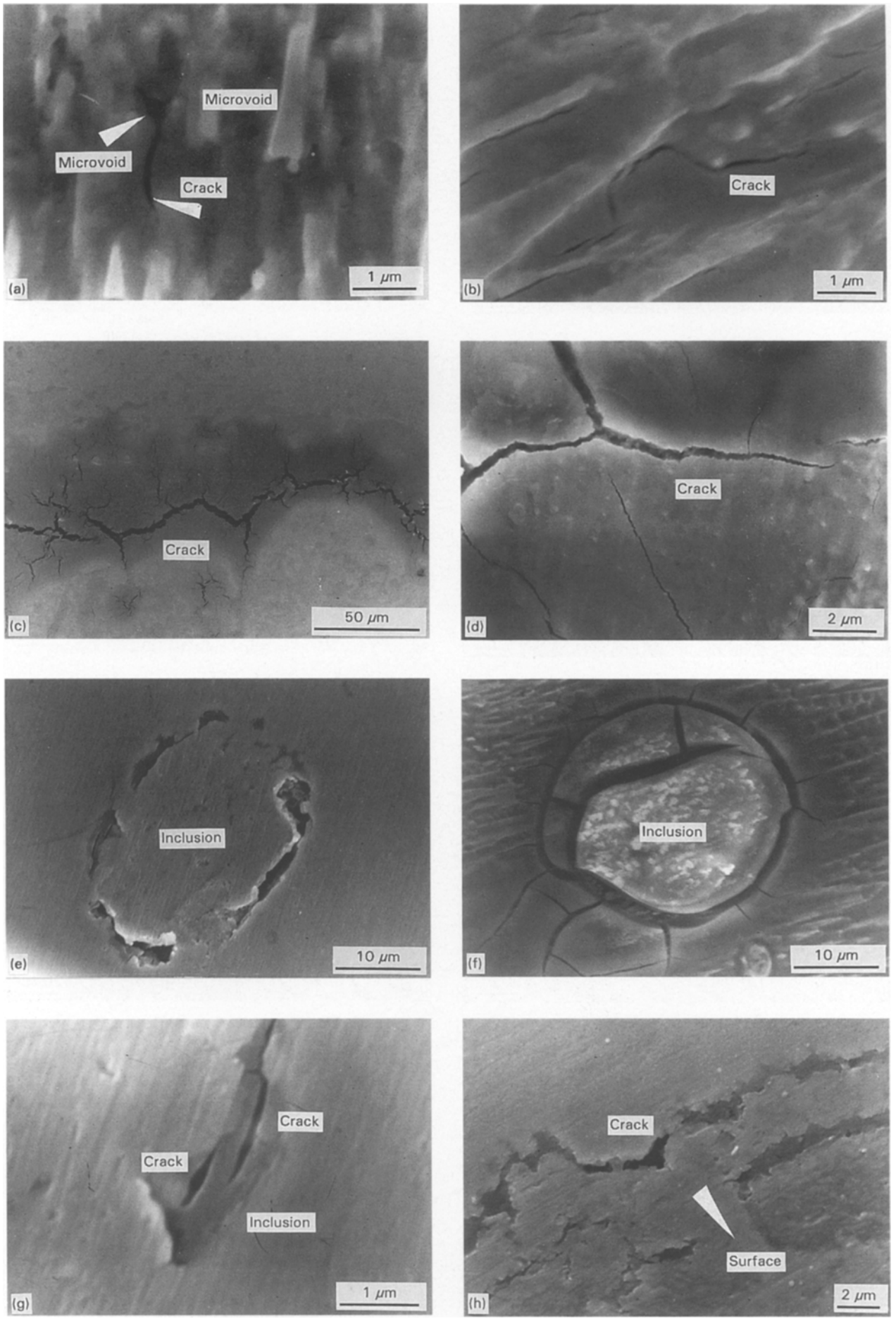

Figure 6 Cross section morphologies of the SMA wire after fatigue testing. (a) Microvoids; (b) crack near martensitic plates; (c) cracks at a location with no martensitic transformation; (d) crack at (c) in detail; (e) cracks between matrix and an inclusion; (f) cracks between matrix and an inclusion and inside the inclusion; (g) microcracks inside of an inclusion, and (h) delamination between core of the wire and the surface layer.

4. Conclusions

1. Heat-treatment procedures were found strongly to influence the properties of the copper-based SMA wires. Due mainly to stabilization of martensite, no reverse transformation was detected for specimens which were directly quenched into water and glycol at room temperature.

2. The degradation life increases with increase in betatizing temperature from 800 °C to 900 °C. The specimens which were heat treated by step quenching showed longer degradation life than those which were directly quenched into ice–water. This advantage, however, disappeared when a high betatizing temperature was applied. The reason for the loss of this advantage may be understood by the dominating effects of grain growth at high temperature.

3. By reducing the duration and temperature of heating, which in turn reduced grain size and minimized vacancy density, degradation life was observed to increase dramatically due to smaller grain size and martensitic plates, and less vacancy concentration.

4. Several types of defect have been observed in the form of microvoids, microcracks, fracture of inclusions, and oxidation of the surface layer. Microvoids and microcracks were normally located near martensitic plates where transformation took place, while large cracks were located at the region where no transformation could be observed. Because of heat treatment, a layer of material with lower zinc and aluminium contents was formed. This layer constituted a discontinuity of martensitic transformation between the layer and the material at the core which led, consequently, to the formation of a crack between the layer and the core. All these defects contributed to the permanent deformation of the SMA wires. In addition, due to the formation of microcracks, stored elastic energy was released leading to the stabilization of martensite.

References

1. MING. H. WU, in "Engineering Aspecs of Shape Memory Alloys", edited by T. W. Duerig, K. N. Melton, D. Stockel and C. W. Wayman (Butterworth-Heinemann, 1990) p. 69.
2. S. MIYAZAKI and K. OTSUKA, *ISIJ Int.* **29** (1989) 353.
3. S. MIYAZAKI, K. OTSUKA, H. SAKAMOTO and K. SHIMIZU, *Trans. Jpn Inst. Metals* **22** (1981) 244.
4. M. SADE, R. RAPACIOLI and M. AHLERS, *Acta Metall.* **33** (1985) 487.
5. J. BEYER, B. KOOPMAN, P. A. BESSELINK and P. F. WILLEMSE, *Mater. Sci. Forum* **56–58** (1990) 773.
6. J. VAN HUMBEECK and R. STALMANS, *ibid.* **56–58** (1990) 405.
7. C. PICORNELL, E. CESARI and M. SADE, *ibid.* **56–58** (1990) 741.
8. J. VAN HUMBEECK, *J. Phys.* **C4** (1991) 189.
9. J. VAN HUMBEECK, J. JANSSEN, M. NGOIE and L. DELAEY, *Script Metall.* **18** (1984) 893.
10. K. SUGIMOTO, K. KAMEI and M. NAKANIWA, in "Engineering Aspects of Shape Memory Alloys", edited by T. W. Duerig, K. N. Melton, D. Stockel and C. M. Wayman (Butterworth-Heinemann, 1990) p. 89.
11. J. PERKINS and R. O. SPONHOLZ, *Metall. Trans.* **15A** (1984) 313.
12. J. JANSSEN, J. VAN HUMBEECK, M. CHANDRASEKARAN, N. MWAMBA and L. DELAEY, *J. Phys.* **C4** (1982) 715.
13. R. STALMANS, J. VAN HUMBEECK and L. DELAEY, *Acta Metall.* **40** (1992) 2921.

Received 16 August 1994
and accepted 8 September 1995